Heteropentadienyl Analogues of Half-Open Ruthenocenes: Metal−Ligand Interactions and Electronic Structure Perturbations

Asha Rajapakshe,[†] M. Angeles Paz-Sandoval,*[,‡] J. Alfredo Gutierrez,[‡] M. Elena Navarro-Clemente,[‡] Patricia Juárez Saavedra,[‡] Nadine E. Gruhn,[†] and Dennis L. Lichtenberger*[,†]

Department of Chemistry, The University of Arizona, Tucson, Arizona 85721, and Departamento de Química, Cinvestav, Av. IPN # 2508, Col. San Pedro Zacatenco, México D. F. 07360, México

Received February 1, 2006

The electronic structures of molecules of the form Cp*Ru(η^5-Pdl) (where Cp* = η^5-pentamethylcyclopentadienyl and Pdl = 2,4-dimethylpentadienyl and various heteropentadienyl ligands, including the azapentadienyl ligand 1-*tert*-butyl-3,5-dimethyl-1-azapentadienyl and the oxopentadienyl ligands 2,4-dimethyl-1-oxopentadienyl and 2,4-di-*tert*-butyl-1-oxopentadienyl) have been investigated using photoelectron spectroscopy and computational methods. The photoelectron spectra of these half-open metallocenes allow direct insight into the bonding capabilities of pentadienyl ligands and the influences of heteroatom substitution on the electronic structure. The number of separate valence ionization bands that are observed corresponds directly to the number of occupied valence metal d orbitals and highest occupied π orbitals of the Cp* and Pdl ligands plus (in the case of the heteropentadienyl ligands) an ionization that derives from the heteroatom (oxygen or nitrogen) lone pair orbital that is in the plane of the ligand. The heteropentadienyl ligand substitution has strong effects on both the ligand- and the metal-based ionizations. Interestingly, the ease of oxidation of the molecules does not follow the expected periodic trend of increasing ionization energy with increasing electronegativity of heteroatom substitution. Density functional calculations give orbital energies and characters for the Cp*Ru(Pdl) molecules in good agreement with those determined by experiment and offer an explanation of the unusual trend in ionization energies with heteroatom substitution. The calculations also show enhanced Ru−cyclopentadienyl bonding accompanying a weakening of Ru−pentadienyl bonding as the pentadienyl ligand becomes more electronegative with heteroatom substitution, which is important for understanding the relative structures and chemical reactivities of heteropentadienyl−metal complexes.

Introduction

The chemistry of pentadienyl (Pdl) ligands opens new avenues of reactivity compared to the chemistry of the well-known cyclopentadienyl (Cp) ligand. A wide variety of Pdl ligands have been synthesized, and studies[1−3] have revealed several unique properties of pentadienyl ligands, leading to numerous possible applications of metal−pentadienyl reaction chemistry.[4−11] One of the interesting chemical perturbations of the pentadienyl ligand is the incorporation of heteroatoms such as oxygen, nitrogen, sulfur, and phosphorus into the pentadienyl fragment.[12−17] In the past, compounds of this class were commonly obtained as unexpected products from various chemical reactions.[12,18−22] Later it was found that such alterations lead to very profound effects in the chemistry, with the heteropentadienyl complexes displaying a much wider range of facile substitutions and reactions.[2,13,23] For example, the oxopentadienyl−metal com-

* To whom correspondence should be addressed. E-mail: dlichten@email.arizona.edu (D.L.L.); mpaz@cinvestav.mx (M.A.P.-S.).
† University of Arizona.
‡ Cinvestav.

(1) Powell, P. *Adv. Organomet. Chem* **1986**, *26*, 125−164.
(2) Ernst, R. D. *Comments Inorg. Chem.* **1999**, *21*, 285−325 and references therein.
(3) Ernst, R. D. *Chem. Rev.* **1988**, *88*, 1255−1291.
(4) Bosch, H. W.; Hund, H.-U.; Nietlispach, D.; Salzer, A. *Organometallics* **1992**, *11*, 2087−2098.
(5) Kralik, M.; Hutchinson, J.; Ernst, R. *J. Am. Chem. Soc.* **1985**, *107*, 8296−8297.
(6) Kulsomphob, V.; Harvey, B.; Arif, A. M.; Ernst, R. D. *Inorg. Chim. Acta* **2002**, *334*, 17−24 and references therein.
(7) Basta, R.; Ernst, R. D.; Arif, A. M. *J. Organomet. Chem.* **2003**, *683*, 64−69.
(8) Severson, S. J.; Cymbaluk, T. H.; Ernst, R.; Higashi, J. M.; Parry, R. *Inorg. Chem.* **1983**, *22*, 3833−3834.
(9) Elschenbroich, C.; Nowotny, M.; Behrendt, A.; Harms, K.; Wocalo, S.; Pebler, J. *J. Am. Chem. Soc.* **1994**, *116*, 6217−6219.
(10) Newbound, T. D.; Freeman, J. W.; Wilson, D. R.; Kralik, M. S.; Patton, A. T.; Campana, C. F.; Ernst, R. D. *Organometallics* **1987**, *6*, 2432−2437.
(11) Koehler, F. H.; Moelle, R.; Strauss, W.; Weber, B.; Gedridge, R. W.; Basta, R.; Trakarnpruk, W.; Tomaszewski, R.; Arif, A. M.; Ernst, R. D. *Organometallics* **2003**, *22*, 1923−1930.
(12) Cheng, M. H.; Cheng, C. Y.; Wang, S. L.; Peng, S. M.; Liu, R. S. *Organometallics* **1990**, *9*, 1853−1861.
(13) Bleeke, J. R. *Organometallics* **2005**, *24*, 5190−5207.
(14) Navarro Clemente, M. E.; Juarez Saavedra, P.; Cervantes Vasquez, M.; Paz-Sandoval, M. A.; Arif, A. M.; Ernst, R. D. *Organometallics* **2002**, *21*, 592−605.
(15) Gutierrez, J. A.; Navarro Clemente, M. E.; Paz-Sandoval, M. A.; Arif, A. M.; Ernst, R. D. *Organometallics* **1999**, *18*, 1068−1079.
(16) Trakarnpruk, W.; Arif, A. M.; Ernst, R. *Organometallics* **1994**, *13*, 2423−2429.
(17) Sanchez-Castro, M. E.; Ramirez-Monroy, A.; Paz-Sandoval, M. A. *Organometallics* **2005**, *24*, 2875−2888.
(18) Bannister, W. D.; Green, M.; Haszeldine, R. N. *J. Chem. Soc. A* **1966**, 194−197.
(19) Bennett, R. L.; Bruce, M. I. *Aust. J. Chem.* **1975**, *28*, 1141.
(20) White, C. T., S. J.; Maitlis, P. M. *J. Organomet. Chem.* **1977**, *134*, 319−325.
(21) Green, M.; Hancock, R. I. *J. Chem. Soc. A* **1968**, 109−113.
(22) Baudry, D.; Daran, J.-C.; Dromzee, Y.; Ephritikhine, M.; Felkin, H.; Jeannin, Y.; Zakrzewski, J. *J. Chem. Soc., Chem. Commun.* **1983**, 813−814.

10.1021/om060100z CCC: $33.50
Publication on Web 03/15/2006

Chart 1

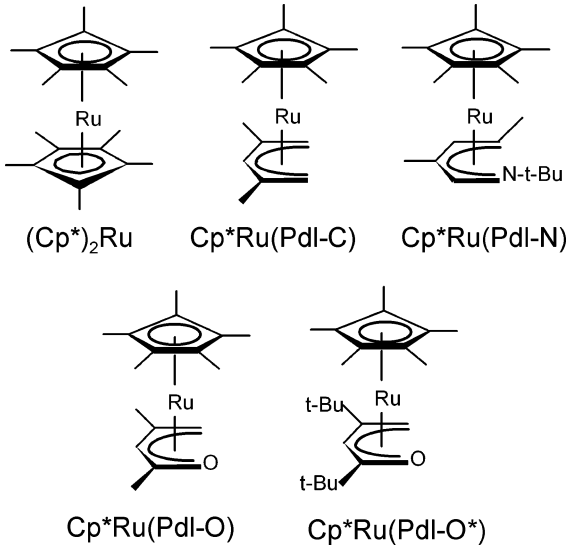

plexes are being utilized as precursors to novel organometallic ring systems such as metallafurans,[24] and they are also being used in the stereoselective functionalization of ketones.[25,26] At least part of the reason for the enhanced reactivity of the heteropentadienyl−metal complexes appears to be more facile interconversions between various bonding modes, such as conversion between η^5 and η^3 bonding to open a coordination site at the metal.[12,14,27,28] The interest in this chemistry has led to improved synthetic routes to transition-metal complexes with heteropentadienyl ligands.[14,15] Recent reviews clearly demonstrate the rich reaction chemistry displayed by these heteropentadienyl−metal complexes.[13,23]

Among the many metal−pentadienyl systems, the Cp*Ru(Pdl) class of compounds supports a rich variety of different pentadienyl ligands, including several heteropentadienyl ligands.[14,15,17] The molecules that are the subject of the present study are depicted in Chart 1, along with a shorthand naming convention that will be used to assist the discussion. These molecules are generally classified as half-open metallocenes. The presence of one open and one closed ring within the same molecule offers the opportunity to compare the bonding of the heteropentadienyl ligands with the bonding of the more familiar cyclopentadienyl ligands to the same metal center.

The relative reactivities of Cp*Ru(Pdl) and Cp*Ru(heteroPdl) toward oxidative addition reactions with $SnCl_4$, Me_2SnCl_2, I_2, and O_2[14] and electrochemical oxidation in acetonitrile[29,30] show that oxopentadienyl complexes (hereafter referred to as Cp*Ru(Pdl-O)) undergo reactions similar to those of the pentadienyl analogue (hereafter referred to as Cp*Ru(Pdl-C)) but are more reactive than the all-carbon species. Also, the Cp*Ru(Pdl-O) molecule undergoes addition reactions with PMe_3 and CO but the Cp*Ru(Pdl-O*) and Cp*Ru(Pdl-C) molecules do not. The chemical reaction of Cp*Ru(Pdl-O) with O_2 results in the oxidation of the Cp* ligand to $C_5Me_4(CHO)$ via a Cp*Ru(η^3-2,4-dimethyl-1-oxopentadienyl)(O_2) complex, which is remarkably stable at room temperature. This complex is useful in selective oxidation reactions, as the activated oxygen molecule can be released under mild conditions. The interesting reaction chemistry displayed by these Cp*Ru(heteroPdl) complexes relative to that of their simple pentadienyl analogues follows from their differences in electronic structure. For example, oxidation chemistry is linked to the energy for ionization and the distribution of charge. While many studies have contributed to the development of facile synthetic routes and reactivities of these heteropentadienyl molecules, the electronic structure effects of the heteropentadienyl ligands in transition-metal systems have been scarcely reported. This study provides a foundation for understanding the electronic structures of representative heteropentadienyl−metal molecules based on the results of gas-phase photoelectron spectroscopy and density functional calculations.

To help understand their valence ionizations and orbital characters, the photoelectron spectra of the Cp*Ru(heteroPdl) molecules are compared with those of their all-carbon analogue Cp*Ru(Pdl-C). Previously, the metal-based ionizations of CpRu(Pdl-C) have been assigned analogously to ferrocene, such that ionizations from the orbitals of Cp*Ru(Pdl-C) that correlate with the metal-based e_{2g} orbitals of ferrocene (primarily the d_{xy} and $d_{x^2-y^2}$ orbitals using the standard coordinate system for metallocenes) were assigned as the first and second ionization bands, followed by an ionization from the orbital of Cp*Ru(Pdl-C) that correlates with the metal-based a_{1g} orbital of ferrocene (primarily the d_{z^2} orbital).[31] However, the present study on Cp*Ru(Pdl-C) reveals that the ionization from the primarily ruthenium d_{z^2} orbital appears between those from the primarily ruthenium d_{xy} and $d_{x^2-y^2}$ orbitals. The spectra show that these half-open ruthenocenes have extremely delocalized electronic structures with a large amount of mixing of the ligand-based Cp* and pentadienyl orbitals. The theoretical calculations of the electronic structure of these molecules agree with the above observations. A fragment analysis within the Hartree−Fock−Roothaan formalism shows a significant enhancement of the donor/acceptor abilities of the Cp* ligand with the Ru center compared to those of heteropentadienyl ligands. This is in agreement with experimental metal−ligand bond distances, which suggest an enhancement of Ru−Cp* bonding with accompanying weakening of the Ru−Pdl bonding as the pentadienyl ligand becomes more electronegative with heteroatom substitution.[14,15,32] Most surprising, the first ionization energy of these molecules does not follow the expected periodic trend with substitution from Pdl-C to Pdl-N to Pdl-O. The principles governing these properties are explored in this work.

Experimental Section

Sample Preparation. The compounds Cp*Ru(Pdl-C),[14,33] Cp*Ru(Pdl-N),[15] Cp*Ru(Pdl-O),[14] and Cp*Ru(Pdl-O*)[14] were prepared according to literature procedures, and the crystal structures are also reported.

Photoelectron Data Collection. Photoelectron spectra were recorded using an instrument that features a 36 cm hemispherical

(23) Paz-Sandoval, M. A.; Rangel-Salas, I. I. *Coord. Chem. Rev.*, in press.
(24) Bleeke, J. R.; New, P. R.; Blanchard, J. M. B.; Haile, T.; Rohde, A. M. *Organometallics* **1995**, *14*, 5127−5137.
(25) Vong, W. J.; Peng, S. M.; Lin, S. H.; Lin, W. J.; Liu, R. S. *J. Am. Chem. Soc.* **1991**, *113*, 573−582.
(26) Pearson, A. J.; Neagu, I. B.; Pinkerton, A. A.; Kirschbaum, K.; Hardie, M. J. *Organometallics* **1997**, *16*, 4346−4354.
(27) Gutierrez Fuentes, J. A. Dissertation, Departamento de Química, Cinvestav, 1999.
(28) Lopez-Martinez, N. I. L.; Paz-Sandoval, M. A. Unpublished results.
(29) Navarro Clemente, M. E.; Chazaro Ruiz, L. F.; Gonzalez, F. J.; Paz-Sandoval, M. A. *J. Electroanal. Chem.* **2000**, *480*, 18−25.
(30) Chazaro Ruiz, L. F.; Gonzalez, F. J.; Paz-Sandoval, M. A. *J. Electroanal. Chem.* **2005**, *585*, 19−27.
(31) Gleiter, R.; Hyla-Kryspin, I.; Ziegler, M. L.; Sergeson, G.; Green, G. C.; Stahl, L.; Ernst, R. D. *Organometallics* **1989**, *8*, 298−306.
(32) Trakarnpruk, W.; Arif, A. M.; Ernst, R. D. *Organometallics* **1992**, *11*, 1686−1692.
(33) Guzei, I. A.; Sanchez-Castro, M. E.; Ramirez-Monroy, A. C.-V., M.; Aleman-Figueroa, I. R.; Paz-Sandoval, M. A. *Inog. Chim. Acta* **2006**, *359*, 701−706.

analyzer[34] and custom-designed photon source, sample cells, and detection and control electronics, as described previously.[35] The ionization energy scale was calibrated using the $^2P_{3/2}$ ionization of argon (15.759 eV) and the $^2E_{1/2}$ ionization of methyl iodide (9.538 eV). The argon $^2P_{3/2}$ ionization also was used as an internal calibration lock of the absolute ionization energy to control spectrometer drift to less than ±0.005 eV throughout data collection. During He I and He II data collection the instrument resolution, measured using the full-width at half-maximum of the argon $^2P_{3/2}$ ionization, was 0.024−0.030 eV. All of the spectra were corrected for the presence of ionizations caused by other emission lines from the discharge source.[36] The He I spectra were corrected for the He Iβ line (1.866 eV higher in energy and 3% of the intensity of the He Iα line), and the He II spectra were corrected for the He IIβ line (7.568 eV higher in energy and 12% of the intensity of the He IIα line). All data also were intensity corrected with an experimentally determined instrument analyzer sensitivity function. In the figures of the data, the vertical length of each data mark represents the experimental variance of that point.[37]

The samples sublimed cleanly, with no visible changes in the spectra during data collection. The sublimation temperatures (in °C, at 10^{-4} Torr) were as follows: Cp*Ru(Pdl-C), 47−68; Cp*Ru(Pdl-N), 50−75; Cp*Ru(Pdl-O), 42−65; Cp*Ru(Pdl-O*), 60−65.

Photoelectron Data Analysis. The valence ionization bands are represented analytically with the best fit of asymmetric Gaussian peaks, as described in more detail elsewhere.[37] The Gaussians are defined with the position, the amplitude, the half-width for the high-binding-energy side of the peak, and the half-width for the low-binding-energy side of the peak. A minimum number of Gaussian peaks is used to model the ionization band contours. The peak positions and half-widths are reproducible to about ±0.02 eV (~3σ level). The parameters describing an individual ionization are less certain when two or more peaks are close in energy and are overlapping. Confidence limits for the relative integrated peak areas are about 5%, with the primary source of uncertainty being the determination of the baseline under the peaks. The baseline is caused by electron scattering and is taken to be linear over the small energy range of these spectra. The total area under a series of overlapping peaks is known with the same confidence, but the individual peak areas are less certain. He II spectra are modeled with the same Gaussian peaks (energies and shapes) as obtained from the analysis of the He I spectra. Only the relative intensities of the Gaussian peaks are allowed to vary to account for the changes in ionization cross sections with excitation photon energy.

Computational Methodology. The BLYP method (Becke exchange[38] and LYP correlation function[39]) at the GGA (generalized gradient approximation) level was used for all calculations that are reported. The atomic orbitals on all centers were described by the TZP (valence triple-ζ with a polarization function) Slater-type basis set that is readily available with the ADF 2004.01 package.[40] A calculation on the Cp*Ru(Pdl-C) molecule with the TZ2P basis set showed very little difference from the TZP basis set. In addition to these calculations, the contributions of scalar relativistic effects were examined by means of the zero order regular approximation (ZORA[41−43]), and the sensitivity of the results to the choice of functional was examined by comparing these calculations with the results using only the Vosko−Wilk−Nusair local correlation approximation without corrections (VWN) and also with the results using the Perdew−Wang exchange-correlation generalized gradient corrections (PW91). References to these methods are available in the ADF documentation.[40] The ZORA contributions had little effect on the optimized geometries or Kohn−Sham orbital energies. The VWN calculations gave slightly better agreement between the pattern of orbital energies and the observed vertical ionization energies, and the PW91 calculations gave slightly better agreement between the optimized geometries and the crystal structures, but the differences are minor and do not affect the ionization assignments or interpretation of the electronic structure. Only the BLYP calculations are reported. The starting *x*, *y*, *z* coordinates for the geometry optimizations for Cp*Ru(Pdl-N) and Cp*Ru(Pdl-O) molecules were from X-ray diffraction experiments.[14,15] For the geometry optimizations the 1s functions on first-row atoms and the functions through 4p on Ru were treated as frozen core, but for the electronic structure analysis all functions were included in the calculations. The orbital plots were generated using the program Molekel.[44] The orbital coefficients and Kohn−Sham Fock matrix obtained from the ADF calculations were transformed to a basis of the ligand fragment orbitals to assist the interpretation of the interactions of the pentadienyl-based orbitals with those of the Cp*Ru fragment.[45,46]

Results

Photoelectron Spectroscopy. The general features of the valence photoelectron spectra of the molecules Cp*Ru(Pdl-C), Cp*Ru(Pdl-N), Cp*Ru(Pdl-O), and Cp*Ru(Pdl-O*) will be introduced, followed by a detailed analysis of the ionization features and trends. The vertical ionization energies and relative areas for the valence ionizations of the molecules under study are given in Table 1.

Before proceeding, it is worth reviewing the photoelectron spectrum of $(Cp^*)_2Ru$. The ionizations of this high-symmetry molecule have been reported and assigned previously,[47] and the general pattern of the ionizations of $(Cp^*)_2Ru$ is similar to that of the molecules studied here, but with additional splittings in the ionizations of the present molecules due to the reduction in symmetry. This similarity can be seen in the comparison of the He I photoelectron spectrum of $(Cp^*)_2Ru$ with that of Cp*Ru(Pdl-C) in Figure 1. Briefly, for $(Cp^*)_2Ru$ the initial ionizations in the low-energy region (6−10 eV) derive from the three occupied metal d orbitals of the low-spin d^6 metal followed at higher ionization energy in this region by ionizations derived from the highest occupied π orbitals (e_1'') of the two Cp* anion ligands. Assuming D_{5d} molecular symmetry for $(Cp^*)_2Ru$ and a coordinate system with the metal *z* axis pointed toward the center of the cyclopentadienyl ring, the metal-based orbitals are $a_{1g}(d_{z^2})$ and $e_{2g}(d_{x^2-y^2}/d_{xy})$ symmetry. In the well-known spectrum

(34) Siegbahn, K.; Nordling, C.; Fahlman, A.; Nordberg, R.; Hamrin, K.; Hedman, J.; Johansson, G.; Bergmark, T.; Karlsson, S. E.; Lindgren, I.; Lindberg, B. *ESCA: Atomic, Molecular and Solid State Structure Studied by Means of Electron*; Almqvist & Wiksells: Uppsala, Sweden, 1967.

(35) Lichtenberger, D. L.; Kellogg, G. E.; Kristofzski, J. G.; Page, D.; Turner, S.; Klinger, G.; Lorenzen. *J. Rev. Sci. Instrum.* **1986**, *57*, 2366.

(36) Turner, D. W.; Baker, C.; Baker, A. D.; Brundle, C. R. *Molecular Photoelectron Spectroscopy*: Wiley-Interscience: London, 1970.

(37) Lichtenberger, D. L.; Copenhaver, A. S. *J. Electron Spectrosc. Relat. Phenom.* **1990**, *50*, 335−352.

(38) Becke, A. D. *Phys. Rev. A: At., Mol., Opt. Phys.* **1988**, *38*, 3098−3100.

(39) Lee, C.; Yang, W.; Parr, R. G. *Phys. Rev. B* **1988**, *37*, 785−789.

(40) ADF2004.01; S.C.M., Theoretical Chemistry, Vrije Universiteit, Amsterdam, The Netherlands (http://www.scm.com).

(41) van Lenthe, E.; Baerends, E. J.; Snijders, J. G. *J. Chem. Phys*. **1993**, *99*, 4597−4610.

(42) van Lenthe. E.; Baerends, E. J.; Snijders, J. G. *J. Chem. Phys*. **1994**, *101*, 9783−9792.

(43) van Lenthe, E.; Ehlers, A.; Baerends, E. J. *J. Chem. Phys*. **1999**, *110*, 8943−8953.

(44) F., P.; Luthi, H. P.; Portmann, S.; Weber, J. Molekel 4.1, 766; Stefan Portmann, H. P. L. C., Ed.; 766; MOLEKEL 4.3; Swiss Center for Scientific Computing, Manno, Switzerland: Manno, Switzerland, 2000−2002.

(45) Senthilkumar, K.; Grozema, F. C.; Bickelhaupt, F. M.; Siebbeles, L. D. A. *J. Chem. Phys* **2003**, *119*, 9809−9817.

(46) Senthilkumar, K.; Grozema, F. C.; Fonseca Guerra, C.; Bickelhaupt, F. M.; Siebbeles, L. D. A. *J. Am. Chem. Soc*. **2003**, *125*, 13658−13659.

(47) Lichtenberger, D. L.; Elkadi, Y.; Gruhn, N. E.; Hughes, R. P.; Curnow, O. J.; Zheng, X. *Organometallics* **1997**, *16*, 5209−5217.

Table 1. Fit Parameters[a] and General Assignments and Labels of Ionizations

position	high, low half-width	rel area[b] He I	rel area[b] He II/He I	label
		Cp*Ru(Pdl-C)		
6.63	0.39, 0.37	1	1	M1
6.84	0.29, 0.16	0.62	1.29	M2
7.44	0.43, 0.37	1.27	0.80	M3
7.73	0.37, 0.25	0.75	0.64	ligand π (L1)
8.01	0.44, 0.31	0.79	0.65	ligand π (L2)
8.92	0.42, 0.25	0.84	0.86	ligand π (L3)
9.24	0.43, 0.31	0.58	0.65	ligand π (L4)
10.08	0.62, 0.20	0.85	0.73	ligand π (L5)
		Cp*Ru(Pdl-N)		
6.08	0.46, 0.33	1	1	M1
6.86	0.27, 0.20	0.70	1.73	M2
7.12	0.27, 0.26	0.66	1.35	M3
7.48	0.41, 0.34	1.10	1.03	ligand π (L1)
8.04	0.36, 0.31	1.20	0.83	N lone pair + ligand π[c]
8.34	0.45, 0.30	0.90	0.78	(N LP and L2)
8.94	0.47, 0.37	0.90	0.82	ligand π (L3)
9.63	0.79, 0.66	1.33	0.62	ligand π (L4)
10.29	0.54, 0.32	1.32	0.59	azadienyl sym π (L5)
		Cp*Ru(Pdl-O)		
6.63	0.43, 0.31	1	1	M1
7.07	0.23, 0.16	0.55	1.47	M2
7.42	0.43, 0.41	1.11	1.07	M3
7.93	0.35, 0.31	0.90	0.71	ligand π (L1)
8.41	0.36, 0.34	1.10	0.72	O lone pair + ligand π[c]
8.75	0.43, 0.25	0.99	0.71	(O LP and L2)
9.46	0.45, 0.37	0.81	0.72	ligand π (L3)
10.04	0.57, 0.40	0.98	0.60	ligand π (L4)
		Cp*Ru(Pdl-O*)		
6.47	0.45, 0.35	1		M1
6.87	0.23, 0.19	0.50		M2
7.11	0.51, 0.32	1.04		M3
7.75	0.44, 0.34	0.96		ligand π (L1)
8.22	0.32, 0.29	0.91		O lone pair + ligand π[c]
8.55	0.48, 0.30	1.17		(O LP and L2)
9.26	0.41, 0.41	0.85		ligand π (L3)
9.74	0.61, 0.47	1.20		ligand π (L4)

[a] All energies in eV. [b] Relative to peak assigned area (=1). [c] Specific assignment based only on the experimental information of the lone pair to one of the ionizations and ligand to the other is not certain.

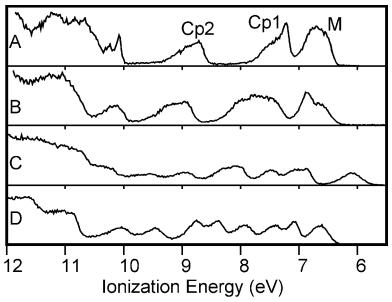

Figure 1. He I photoelectron spectra of (A) $(Cp^*)_2Ru$, (B) Cp*Ru(Pdl-C), (C) Cp*Ru(Pdl-N), and (D) Cp*Ru(Pdl-O).

of ferrocene (not shown),[48] the initial portion of the metal ionization region is attributed to the $^2E_{2g}$ positive ion state and the sharp shoulder to higher binding energy is ascribed to the $^2A_{1g}$ ion state. The metal band of $(Cp^*)_2Ru$ has a more complicated structure than that of ferrocene, due to spin−orbit splitting of the $^2E_{2g}$ positive ion state into two states. Close-up examination of the band from 6 to 7 eV in the spectrum of $(Cp^*)_2Ru$ in a previous report[47] revealed three overlapping peaks, with the center peak assigned to the $^2A_{1g}$ ion state and the outer peaks in this band assigned to the spin−orbit split states from the $^2E_{2g}$ configuration.

As for the Cp* π ionizations of $(Cp^*)_2Ru$ in the region from 7 to 9.5 eV, the e_{1g} orbital (from combination of the e_1'' orbitals of the two Cp* ligands) is the correct symmetry to interact with the metal d orbitals, while the e_{1u} combination is not. The metal−ligand bonding stabilizes the observed $^2E_{1g}$ ion state of the molecule (ionization band labeled Cp2 in Figure 1A) by about 1.5 eV relative to the $^2E_{1u}$ ion state (Cp1 in Figure 1A), indicating significantly delocalized mixing.

The ligand-based a_{1g} and a_{2u} orbitals (combinations of the totally π bonding a_1'' orbitals of the Cp* anions) are fairly stable, and their ionizations are not observed in this energy region. The sharp ionizations just above 10 eV in the spectrum of $(Cp^*)_2Ru$ are associated with a particular symmetry combination of the methyl C−H bonds. Valence ionizations at higher energy are from the C−C and C−H σ bonds and the most stable π bond orbitals of Cp*.

As mentioned, the ionizations of the half-open metallocenes in this study are similar to those of $(Cp^*)_2Ru$, but the degeneracy of the ion states is split, due to the lower symmetry of the molecules. In addition, the heteropentadienyl complexes also contain an ionization in this region that derives from the oxygen or nitrogen p orbital (depending on the heteroatom substitution) that is in the plane of the ligand. This orbital will be referred to as the in-plane lone pair or simply the lone pair. The ionizations of each of these molecules will now be considered in more detail.

Cp*Ru(Pdl-C). Assignment of the ionization bands is aided by comparison of the relative ionization peak intensities in the He I and He II spectra, which provides insight into the atomic character associated with each ionization band.[49,50] The relative ionization intensities of the peaks in the He I and He II spectra are listed in Table 1. For visual comparison, the He I and He II close-up spectra of this pentadienyl molecule are shown in Figure S1 in the Supporting Information. Briefly, after account is taken for analyzer sensitivity, resolution, and higher energy photons in the discharge source, the photoelectron spectra obtained with He IIα photons differ from those obtained with He Iα photons only in the relative intensities of the ionization bands. The change in relative intensities as a function of the change in source photon energy from He Iα to He IIα is due primarily to the different inherent photoionization cross-sections of the atomic orbitals.[50] The theoretical photoionization cross-section of Ru 4d atomic orbitals decreases by a factor of 1.25 for He II excitation compared to He I excitation,[51] while the photoionization cross-section for C 2p orbitals decreases by a factor of 3. As a result, the ionization bands arising from predominantly metal character should increase relative to the bands with ligand (carbon) character when the He II spectrum is compared to the He I spectrum. The amount of the metal−ligand mixing modifies the relative intensity changes according to the character of the molecular orbital. The metal bands are labeled as M1, M2, and M3 for the purpose of discussion. The metal bands increase in relative area compared to the rest when He II photons are used instead of He I photons. The increase of M2 is substantial, indicating a relatively pure metal orbital, while the increases of M1 and M3 are less noticeable, indicating significant mixing of M1 and M3 with the ligand orbitals. Both

(48) Cauletti, C.; Green, J. C.; Kelly, M. R.; Powell, P.; Van Tilborg, J.; Robbins, J.; Smart, J. *J. Electron Spectrosc. Relat. Phenom.* **1980**, *19*, 327−353.
(49) Green, J. C. *Acc. Chem. Res.* **1994**, *27*, 131−137.
(50) Green, J. C.; Decleva, P. *Coord. Chem. Rev.* **2005**, 249, 209−228.
(51) Yeh, J. J.; Lindau, I. *At. Data Nucl. Data* **1985**, *32*, 1.

observations have important implications for the interpretation of the bonding and electronic structure.

The metal-based ionizations of the related molecule (η^5-C_5H_5)(η^5-2,4-dimethylpentadienyl)ruthenium (CpRu(Pdl-C) in the present notation) have been assigned previously by Gleiter et al.[31] similarly to the assignment of the metal-based ionizations of ferrocene, with the first two bands seen in the spectrum attributed to ionization from the predominantly $d_{x^2-y^2}$ and d_{xy} orbitals and the third ionization band appearing at higher energy ascribed to ionization from the predominantly d_{z^2} orbital. A similar assignment would be expected for the Cp*Ru(Pdl-C) molecule, since the only difference between the two molecules is permethylation of the cyclopentadienyl ring. However, the He I/He II comparison of the ionizations of Cp*Ru(Pdl-C) indicates that the previous assignment is not correct for the ionizations of these molecules. The dramatic increase in the relative intensity of the M2 band (refer to He II/He I relative areas in Table 1) leads to the assignment of that band to the nonbonding metal d_{z^2} (similar to the $^2A_{1g}$ state in ferrocene), because it is expected to have the greatest metal character. The M1 and M3 bands are attributed to ionizations primarily from the $d_{x^2-y^2}$ and d_{xy} orbitals that are derived from the e_{2g} type MO of ferrocene, although which is which cannot be determined solely from these photoelectron spectra.[52] The greater splitting of the e_{2g} band compared to that in ruthenocene is due to the lowered symmetry of the pentadienyl molecule. The spectra of the subsequent molecules and the computational models to be discussed lend additional support to this assignment and interpretation.

The intensities of the ionization bands that occur at energies above M3 in Table 1 generally decrease relative to the bands below M3, supporting the assignment of the bands above M3 to ionizations containing generally more ligand character and less metal character. Two ionization shoulders labeled as L1 and L2 in Table 1 are observed in addition to the ionization labeled M3 in the band around 8 eV. The band at 9 eV requires two peaks (L3 and L4) to model the contour, and the band near 10 eV (L5) requires only one peak. On the basis of the spectrum of $(Cp^*)_2Ru$, it can be anticipated that the ionization bands L1, L2, L3, and L4 each contain two ionizations of mixed Cp* and 2,4-dimethylpentadienyl character. The exact assignment of these bands to their corresponding molecular orbitals is difficult because of the mixing between both ligands and the metal. The description of these ionizations is assisted by the ADF calculations performed on this molecule that will be described later.

Cp*Ru(Pdl-N). The assignments of the ionization bands of this molecule are similar to those of the pentadienyl analogue. The He I and He II close-up spectra of Cp*Ru(Pdl-N) are shown in Figure S2 (Supporting Information). The first three bands are predominantly Ru 4d in character, and the ionizations at higher energy are ligand-based. The similar characters of the M1 and M3 ionizations and the relative intensity changes from He I to He II excitation are more apparent than for Cp*Ru(Pdl-C) because of the greater separation of the metal-based ionizations from the ligand-based ionizations. From comparison with the spectrum of Cp*Ru(Pdl-C), an additional peak in the band from 8 to 8.5 eV derives from the presence of the nitrogen lone pair. The electronegative nitrogen in the pentadienyl ligand is expected to stabilize the ionizations of Cp*Ru(Pdl-N) relative to those of the Cp*Ru(Pdl-C) pentadienyl molecule. This is generally true for the ligand-based ionizations, although the shifts are uneven, and the first ligand-based ionization, L1, actually shifts to lower ionization energy by about 0.25 eV compared to the corresponding ionization of Cp*Ru(Pdl-C). Interestingly, the metal-based ionizations M1 and M3 shift even more to lower ionization energy. The metal-based first ionization, M1, is affected the most, decreasing by about 0.55 eV, indicating considerable energy differences in the HOMO's. This unusual result will be addressed in more detail in the Discussion.

Cp*Ru(Pdl-O). The assignments of the ionization bands of this molecule are again similar to those of the Cp*Ru(Pdl-C) analogue, but in this case there is an even more clear separation of the individual ionization peaks. The first three ionizations are the metal-based ionizations, followed by five ionizations arising from the four ligand-based π orbitals and the additional oxygen lone pair orbital. The He I and He II photoelectron spectra of the oxopentadienyl molecule from 6 to 11 eV are shown in Figure S3 (Supporting Information), and the relevant information on ionization intensities is collected in Table 1. The increase in the intensity of the M3 ionization in the He II spectrum relative to the ionizations at higher energy is seen most clearly in this case. On the basis of the observation that the oxygen lone pair ionization in acetone appears at 9.70 eV,[53] and taking into account the formal negative charge on the oxopentadienyl ligand, the fifth or sixth ionization bands in the photoelectron spectrum most likely have substantial oxygen lone pair character.

The substitution of the oxygen atom for a CH_2 group in the pentadienyl ligand is again expected to stabilize all of the ionizations with pentadienyl character, more so than the nitrogen atom substitution. When the ionizations of Cp*Ru(Pdl-C) and Cp*Ru(Pdl-O) are compared (Table 1 and Figure S4 (Supporting Information)), it is evident that all of the ligand-based ionizations in the Cp*Ru(Pdl-O) molecule are stabilized relative to the metal-based ionizations, indicating that there is strong mixing between the Cp* and 2,4-dimethyl-1-oxopentadienyl orbitals. The nonbonding M2 ionization is stabilized by about 0.2 eV in the oxopentadienyl molecule compared to that of the pentadienyl molecule, due to the charge effects from the electronegative oxygen atom. However, the energies of the metal-based M1 and M3 ionizations are not affected by the oxo substitution. This again is a topic for discussion.

Cp*Ru(Pdl-O*). The effect of alkyl group substitution on the oxopentadienyl ligand is studied using Cp*Ru(Pdl-O*) as a comparison to the 2,4-dimethyl-1-oxopentadienyl molecule. The relative shifts of the valence metal-based and pentadienyl-based ionizations give an indication of the overall electronic effects of methyl and *tert*-butyl substitution on the oxopentadienyl ligand. The ionizations corresponding to the oxopentadienyl ligand are expected to destabilize the most upon *tert*-butyl substitution compared to methyl substitution. These shifts are observed in the ionization energies listed in Table 1, and visual comparison of the He I spectrum of the *tert*-butyloxopentadienyl molecule with that of the methyloxopentadienyl molecule is shown in Figure S4 (Supporting Information). All of the metal-based and ligand-based ionizations of the *tert*-butyloxopentadienyl group have been shifted to lower ionization energy relative to those of the oxopentadienyl molecule, and M1 and M3 are shifted substantially. This is another indication that there is an extensive mixing of metal and ligand orbitals (both Cp* and pentadienyl ligand) in these molecules.

Computational Results. Orbital surface plots and Kohn−Sham orbital energies for the eight highest occupied molecular orbitals and the corresponding photoelectron ionization bands

(52) Bohm, M. C.; Gleiter, R. *Theor. Chim. Acta* **1981**, *59*, 127, 153.

(53) Kimula, K.; Katsumata, Y.; Achiba, Y.; Yamazaki, T. *Handbook of He I Photoelectron Spectra of Fundamental Organic Molecules*; Scientific Societies Press: Tokyo, Japan, 1980.

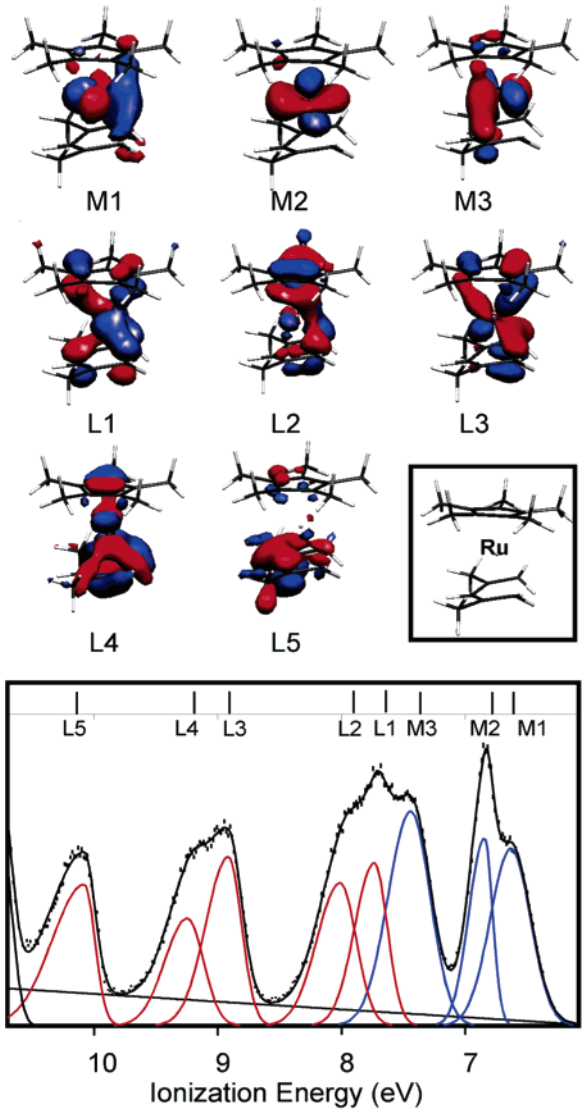

Figure 2. Comparison of ionization bands with molecular orbital surfaces (±0.05) for the frontier orbitals of Cp*Ru(Pdl-C). The vertical lines with labels shown at the top of the spectrum represent the calculated Kohn−Sham orbital energies with the energy of the HOMO aligned with the first ionization.

for the Cp*Ru(Pdl-C) molecule are shown in Figure 2. The computational results agree with the primary features in the experimental photoelectron spectra. The energy spacings of the calculated orbital energies for the valence region of these molecules match the spacings of the vertical ionization energies in this energy region extremely well, and the characters of the orbitals agree with the characters indicated by the experiment. The first three orbitals (M1−M3) are predominantly Ru 4d in character, M2 being predominantly the $4d_{z^2}$ orbital with very little ligand character on the basis of the calculations, in agreement with the intensity differences in the He I and He II experiments. The calculations for the pentadienyl molecule show that the M1 and M3 Kohn−Sham orbitals are metal-based in character and have greater mixing from the ligand orbitals. The next four orbitals from the calculations are primarily Cp* and 2,4-dimethylpentadienyl ligand-based and have a significant amount of mixing in their molecular orbitals with each other and with metal-based orbitals. The last MO shown in Figure 2 is the symmetric π combination of the pentadienyl ligand fragment, which remains largely localized on this ligand.

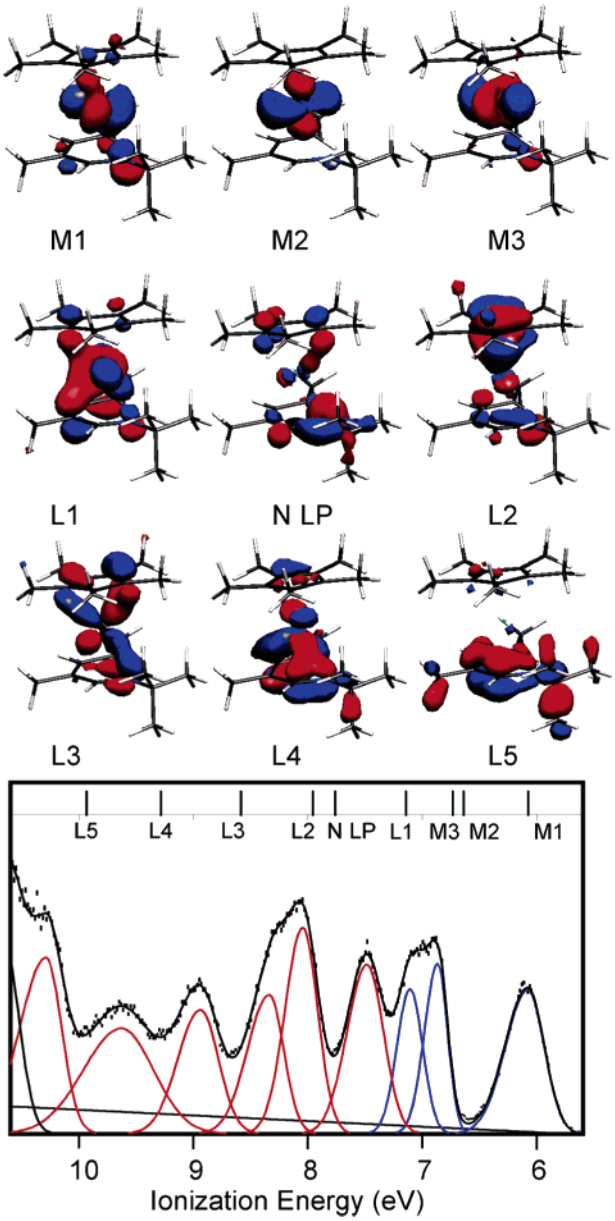

Figure 3. Comparison of ionization bands with molecular orbital surfaces (±0.05) for the frontier orbitals of Cp*Ru(Pdl-N). The vertical lines shown at the top of the spectrum with labels represent the calculated Kohn−Sham orbital energies with the energy of the HOMO aligned with the first ionization. The N-*t*-Bu group is located in the lower right corner of the molecule.

For the orbitals of the azapentadienyl complex, shown in Figure 3, the first three orbitals are primarily Ru 4d in character with nonbonding M2. The fourth MO, labeled L1, is delocalized over the Cp* and azapentadienyl ligand and metal orbitals. The fifth MO is primarily nitrogen (in plane lone pair) in character and is labeled as N LP. In the figure, this MO is correlated with the fifth ionization band in the photoelectron spectrum of the azapentadienyl molecule, but it is not possible to make a definitive assignment of this ionization in this region by the He I and He II comparison, because all of the ligand-based MO's have substantial nitrogen character in them. The sixth and seventh MO's have both Cp* and azapentadienyl ligand character with some metal character. The eighth MO shown in Figure 3 is predominantly azapentadienyl in character, and the last MO shown is a representation of the symmetric π combination of the azapentadienyl ligand fragment.

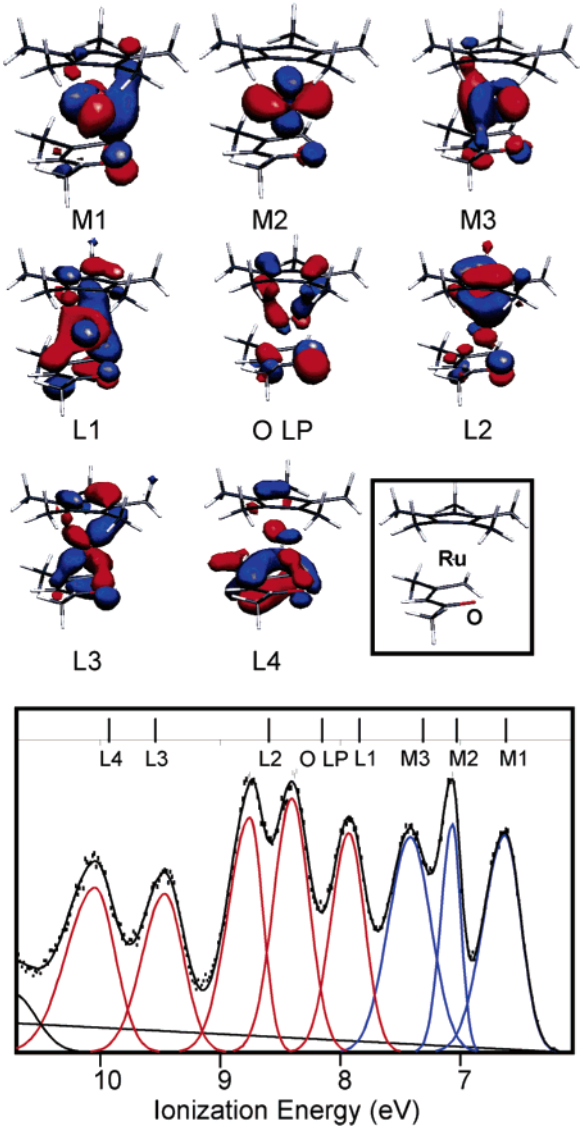

Figure 4. Comparison of experimental ionization bands with calculated molecular orbital surfaces (±0.05) for the frontier orbitals of Cp*Ru(Pdl-O). The vertical lines shown at the top of the spectrum with labels represent the calculated Kohn−Sham orbital energies with the energy of the HOMO aligned with the first ionization.

The oxopentadienyl molecule shows primary features similar to those of the azapentadienyl complex. The fifth MO labeled as O LP has substantial oxygen in-plane orbital character, which correlates with the fifth ionization band in Figure 4. However, again the mixing of oxygen character with all the ligand orbitalsmakes it difficult to assign this ionization precisely in the spectrum on the basis of He I and He II comparisons. The most stable π combination of the oxopentadienyl ligand ionizes at higher energy and is not shown in the valence ionization region in Figure 4.

The calculated Kohn−Sham orbital energies follow a trend between the molecules similar to the trend observed in the experimental ionization energies. For example, the first ionization energies of the pentadienyl and oxopentadienyl molecules are calculated to be approximately the same, and that of the azapentadienyl molecule is calculated to be destabilized to considerably lower ionization energy compared to the other molecules.

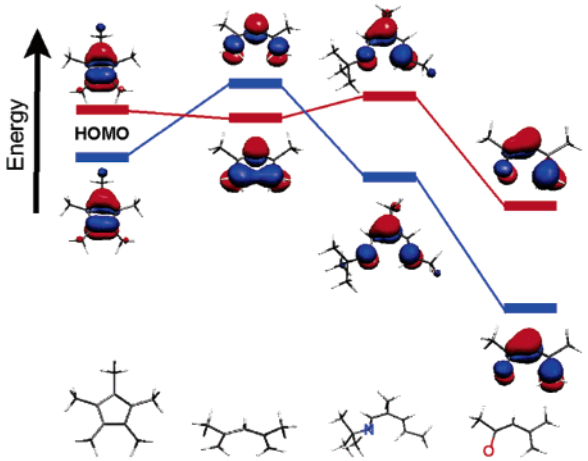

Figure 5. Correlation among the HOMO energies (eV) of Cp*, Pdl-C, Pdl-N, and Pdl-O ligands. The blue line represents the HOMO energies for the optimized geometries of the free anions, and the red line represents the HOMO energies of the free anions constrained to the geometries when bound to the metal.

Discussion

The photoelectron spectra of this series of heteropentadienyl-substituted half-open ruthenocenes display an unusual trend with heteroatom substitution. Chemical substitutions in molecules with atoms and functional groups of increasing electronegativity generally result in increasing ionization energies. In the series of half-open ruthenocenes with the pentadienyl ligands Pdl-C, Pdl-N, and Pdl-O one would expect the ionization energies to increase in the order Pdl-C < Pdl-N < Pdl-O, but this is not observed for the first ionization and several of the other ionizations of these molecules. Although this order is not obtained for the metal complexes, this order is obtained for the calculated orbital energies of the ligands themselves, as shown in Figure 5. This figure shows the correlation between the highest occupied π molecular orbitals of Cp*, 2,4-dimethylpentadienyl, 1-*tert*-butyl-3,5-dimethyl-1-azapentadienyl, and 2,4-dimethyl-1-oxopentadienyl based on density functional theory calculations of the ligands. The orbital energies depicted in blue are for the free ligand anions at their optimized geometries. One of the degenerate e_1'' orbitals of the Cp* anion is shown on the left of Figure 5. The next column shows the corresponding HOMO energy and orbital of the 2,4-dimethylpentadienyl anion. The bonding stabilization this orbital experiences in Cp* is lost with the increased separation between the terminal carbon atoms of 2,4-dimethylpentadienyl, and the orbital energy is less stable. This shift is partially counterbalanced by the smaller number of methyl groups in 2,4-dimethylpentadienyl compared to that in Cp*, so that the energy difference between the HOMO's of Cp* and 2,4-dimethylpentadienyl is smaller than would occur otherwise. This energy similarity contributes to the large degree of mixing between the highest orbitals of the pentadienyls and Cp* in the molecules. The energies of the highest occupied orbitals of the Pdl-N anion and the Pdl-O anion show the steady stabilization of orbital energies with increasing electronegativity of the groups in the terminal positions of the pentadienyls, as expected.

A close-up view of metal-based ionizations for the pentadienyl molecules, shown in Figure 6, makes clear the unusual pattern of the first ionization energies. The correlation of all of the measured valence ionization energies of these molecules is shown in Figure 7. The M2 ionization approximately follows the trend of higher ionization energy with increasing electrone-

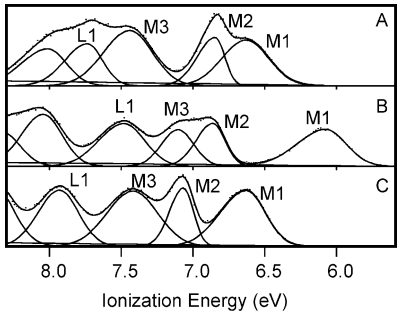

Figure 6. Close-up spectra of the metal bands of (A) Cp*Ru(Pdl-C), (B) Cp*Ru(Pdl-N), and (C) Cp*Ru(Pdl-O).

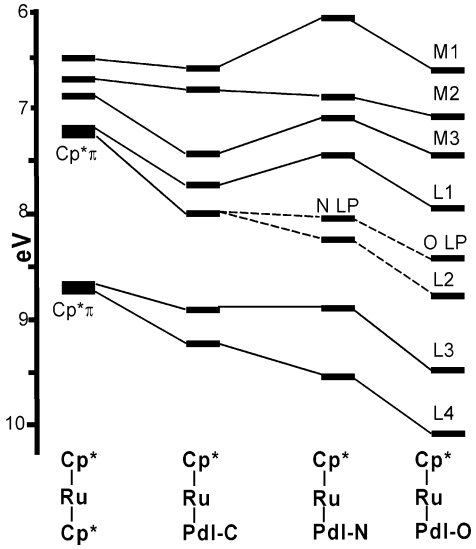

Figure 7. Correlation diagram illustrating the shifts of ionization energies observed upon substitution of Cp* with η^5-2,4-dimethylpentadienyl, η^5-1-*tert*-butyl-3,5-dimethyl-1-azapentadienyl, and η^5-2,4-dimethyl-1-oxopentadienyl. Specific assignment of the lone pair to one of the ionizations and ligand (L2) to the other is not certain.

gativity, occurring at approximately 0.2 eV higher ionization energy for the oxopentadienyl complex compared to the energies of the other two. The shift of the M2 ionization from the pentadienyl to the azapentadienyl complex is only slight, which may be a consequence of the added inductive donation effect of the *t*-Bu group bound to the nitrogen atom of the azapentadienyl. The M2 orbital is the most pure of the metal-based orbitals, and this probably accounts for this ionization most closely following the electronegativity trend. The shifts of the M1 and M3 ionization energies observed for these half-open ruthenocenes clearly do not follow the periodic trend of electronegativities with the heteroatom substitution, and the deviation of the first ionization from this trend is the most dramatic, with the first ionization of the Pdl-N molecule occurring at substantially lower energy than the first ionization of the other molecules. The trend of the first ionization energy from Pdl-N to Pdl-O is as expected, but the first ionization energy of the Pdl-C molecule is abnormally high in this series.

The Kohn−Sham orbital energies from the calculations reproduce these trends and offer an explanation for the unusual behavior. The lower first ionization energy of the Pdl-N molecule compared to that of the Pdl-C molecule might at first thought be attributed to the inductive and/or steric effects of the *t*-Bu substitution on the nitrogen atom. However, replacing the *t*-Bu group with a hydrogen atom in the calculations produces the same trend in the ionization energies, with only a slight (∼0.1 eV) stabilization of the first ionization of the Pdl-N molecule. An understanding of the trend in the first ionization energies of the molecules begins with a more complete understanding of the energies of the highest occupied orbitals of the ligands. When the ligands bind to the metal, they undergo geometric distortions to optimize the bonding and minimize steric repulsions. The Pdl-C ligand binds most strongly to the metal (vide infra) and undergoes the greatest distortion. This distortion and its effect on the highest occupied orbital of the ligand are shown in Figure 5, in which the orbital energies for the ligands at their coordinated geometries are depicted in red. In comparison to the free Pdl-C anion, the coordinated Pdl-C ligand has undergone a distortion in which the terminal carbon atoms move ∼0.5 Å closer to each other and the terminal CH_2 groups twist ∼50° to improve the terminal C pπ interaction with the metal. The result on the ligand is that some bonding character is reintroduced between the terminal carbon atoms, as shown by the orbital surface (the lower orbital in the second column) in Figure 5. Consequently, the highest occupied orbital of Pdl-C is stabilized at the geometry of the coordinated ligand (shown in red) relative to the same orbital of the free ligand (shown in blue). Pdl-C is the only ligand of the group for which the HOMO is stabilized in the coordinated geometry relative to the free ligand, and this orbital becomes more stable than the corresponding orbital of both Cp* and Pdl-N. This interaction dominates the charge effects on the ligand HOMO energy from the change in electronegativity from Pdl-C to Pdl-N. Proceeding to Pdl-O in Figure 5, the electronegativity change dominates and the HOMO of Pdl-O is the most stable of the HOMO's of these ligands. This pattern with only slight adjustments (due to the charge and overlap interactions in the molecule) is reflected in the trend of the experimentally observed L1 ionization energies in Figure 7.

Because of the delocalized electronic structure of these molecules, the perturbations in the electronic structures of the heteropentadienyl ligands are felt throughout the molecules. The M1 and M3 ionizations reflect the same general pattern in ionization energies as the L1 ionization, as tempered by the energy proximity and overlap with the ligand orbitals. The L1 ionization is closest in energy to the metal ionizations in the case of the Pdl-N molecule, and the calculations show that the M1 orbital of this molecule has the most pentadienyl character (29%) and the least metal character (58%) of these molecules. The corresponding values for the Pdl-C molecule are 12% and 77%, and the corresponding values for the Pdl-O molecule are intermediate at 21% and 66%. Thus, the first ionization of the Pdl-N molecule is shifted most to lower ionization energy.

Table 2. Calculated Total Donor and Acceptor Abilities for Cp* and Pentadienyl Ligands and the Calculated Mayer Ru−L Bond Order.

	Cp*Ru-(Pdl-C)		Cp*Ru-(Pdl-N)		Cp*Ru-(Pdl-O)	
	Cp*	Pdl-C	Cp*	Pdl-N	Cp*	Pdl-O
total donor ability	1.20	1.28	1.23	1.14	1.32	1.03
total acceptor ability	0.38	0.62	0.46	0.47	0.45	0.51
Mayer Ru−L bond order	1.88	2.32	2.09	1.98	2.15	1.95

Donor/Acceptor Abilities of Pentadienyl Ligands. The crystallographic data suggest an enhancement of the Ru−Cp* bonding, with accompanying weakening of the Ru−Pdl bonding, as the pentadienyl ligand becomes more electronegative.[14,15,32,33] The calculated donor abilities of the heteropentadienyl ligands in these complexes follow the expected trend of decreasing donor ability with increasing electronegativity of the heteroatom substitution, as shown in Table 2. At the same time, and not necessarily expected on the basis of electronegativity, the

heteropentadienyl ligands are calculated to be poorer acceptor ligands than pentadienyl. As a consequence, the heteropentadienyl ligands bind less strongly to the Ru center in these molecules than the pentadienyl ligand. The acceptor and the donor ability of Cp* increases on going from pentadienyl to heteropentadienyl molecules, indicating a significant enhancement of Ru−Cp* bonding at the expense of Ru−pentadienyl bonding. The calculated Mayer Ru−ligand bond orders[54] reflect the same trend, as shown in Table 2. The Mayer Ru−ligand bond orders have values near 2 because, although the ligands are formally six-electron donors representing a triple bond, the totally symmetric π orbitals of the ligands have poor overlap with metal d orbitals and are substantially more stable in energy and, therefore, are not effective donors. Donation from the two highest occupied π orbitals of the pentadienyls accounts for most of the Mayer double-bond order. The Pdl-C ligand bonds most strongly, and as the bonding of the pentadienyl weakens from the Pdl-N to the Pdl-O ligands, the bonding of the Cp* to the metal in these molecules strengthens. The Pdl-C ligand is the only pentadienyl of this group that bonds to the metal more strongly than Cp*. The calculations are thus seen to reproduce the experimentally observed enhancement of Ru−cyclopentadienyl bonding accompanying a weakening of Ru−pentadienyl bonding, as the pentadienyl ligand becomes more electronegative with heteroatom substitution. These indications of relative bond strengths, along with the additional stabilization of the pentadienyl complex observed in the valence ionizations, show that the heteropentadienyl complexes should have enhanced reactivities.

A substantial part of the weakening of the Ru−heteropentadienyl bond is directly due to the poorer bonding between the heteroatom and the metal. The Ru−O Mayer bond order is only 0.38 in the Pdl-O complex compared to a Ru−N bond order of 0.44 in the Pdl-N complex and a Ru−C terminal bond order of 0.57 in the Pdl-C complex, consistent with atomic size and electronegativity.

Insights into the Reactivities of Heteropentadienyl−Metal Complexes. The characteristic features of electronic structure and bonding uncovered by the present study of half-open heteropentadienyl−ruthenium molecules provide a framework for understanding the chemistry of these and other heteropentadienyl−metal systems. The photoelectron spectra of these molecules are particularly informative, because identifiable ionization peaks are observed corresponding to each of the expected valence ionization states of these molecules. A correlation diagram of the shifts in ionization energies upon ligand substitution is shown in Figure 7. Several important points are evident from this diagram. The breakdown of degeneracy of the Cp* π ionizations upon substitution of a pentadienyl ligand in place of a Cp* ligand is one indication of the delocalized electronic structure across the ligands of these complexes. Another indication of substantial mixing and delocalization throughout the molecules is the observation that all of the ionizations are perturbed when a heteroatom is substituted for a CH_2 group. The assignment of a specific ionization in the spectra of the heteropentadienyl molecules to the heteroatom in-plane lone pair ionization is not possible on the basis of the He I/He II comparison because of the extensive mixing of ligand character in all of the orbitals. Looked at another way, the substantial coupling and mixing between all of the valence orbitals is one reason that separated ionization peaks are observed for all of the ion states.

The M1 and M3 ionizations as well as the first ligand-based ionization L1 of Cp*Ru(Pdl-C) show an extra degree of stabilization that is out of line with the other molecules in this study. The higher than expected ionization energies of Cp*Ru(Pdl-C) follow from the stronger bonding of the pentadienyl ligand to the metal, the greater distortion of the pentadienyl ligand in bonding to the metal, and the increased bonding character between the terminal carbon atoms of the pentadienyl when bound to the metal center. As a consequence of the orbital mixing and in contrast to group electronegativity, the Cp*Ru(Pdl-N) complex has the lowest first ionization energy of this group of molecules. Whereas the Pdl-C ligand has the strongest bonding to the metal, the Pdl-O ligand has the weakest bonding to the metal, and is most susceptible to conversion from η^5 to η^3 bonding to the metal. For example, the Cp*Ru(Pdl-O) molecule undergoes addition reactions with PMe_3 and CO in which the Pdl-O ligand rearranges to η^3-allyl bonding to the metal and the PMe_3 or CO ligand binds to the vacated coordination site as shown by

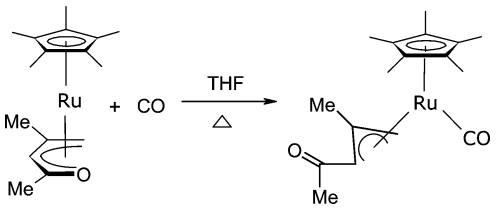

The rearrangement of the Pdl-O ligand to η^3-allyl bonding is favored in general by the weaker η^5 Ru−Pdl-O ligand bonding and in particular by the weaker Ru−O and Ru−C2 (carbon adjacent to the heteroatom) bonding of the Pdl-O ligand compared to that of the other ligands. The Cp*Ru(Pdl-C) complex, with stronger η^5 bonding of the Pdl-C ligand to the metal center, does not undergo this reaction. The reactivity of the Cp*Ru(Pdl-O*) complex suggests that the electronic effects are more important than the steric effects for this molecule. The bulky *t*-Bu groups on Pdl-O* might favor the opening up of the ligand to the η^3-allyl arrangement with reduced steric congestion, but the increased electron donor ability of the ligand moves the orbital energies and ionizations to lower energy and increases the bonding to the Ru center, disfavoring the η^5 to η^3 rearrangement. The Cp*Ru(Pdl-O*) molecule does not add PMe_3 or CO.

The electronic structure and bonding features of these heteropentadienyl complexes help in understanding the properties of other transition-metal−heteropentadienyl complexes. For example, the reactivities displayed by (heteropentadienyl)Mn(CO)$_3$ molecules are consistent with the electronic structure and bonding properties uncovered in this study, even though the electronic structure of the Mn(CO)$_3$ fragment is much different from that of the Cp*Ru fragment.[12] For instance, the carbonyl stretching frequencies of the (azapentadienyl)Mn(CO)$_3$ molecule are lower than those of the corresponding pentadienyl and oxopentadienyl molecules, reflecting the greater electron richness that results from the lower ionization energy of the HOMO of the azapentadienyl. In this case the lone pair of the nitrogen atom donates so strongly to the metal that it disrupts the fully delocalized η^5-azapentadienyl bonding and forms an η^1-N, η^3-allyl-type structure.[27,28] The (oxopentadienyl)Mn(CO)$_3$ complex readily undergoes phosphine addition reactions to form (η^3-oxopentadienyl)Mn(CO)$_3$PR$_3$, while the corresponding azapentadienyl−metal complex is inert, reflecting the weaker metal−oxygen bonding compared to the metal−nitrogen bonding.[12]

(54) Mayer, I. *Chem. Phys. Lett.* **1983**, *97*, 270−274.

The extensive orbital interactions in these systems help create a fluid electron density such that chemical perturbations of the heteropentadienyls are felt throughout the molecules and can have unexpected consequences. The availability of facile transformations between η^5 and η^3 bonding modes, which opens numerous reaction possibilities, is linked to weak donor/acceptor capabilities of the heteropentadienyl ligand, suggesting an approach to tuning the reactivity. These insights into the influences of electronic structure and bonding on the reactivities of heteropentadienyl−metal complexes that are known so far suggest much promise for the continuing development of heteropentadienyl−metal chemistry.

Acknowledgment is made to the donors of the Petroleum Research Fund, administered by the American Chemical Society, for partial support of this research. D.L.L. thanks the National Science Foundation (Grant No. CHE0416004), and A.R. acknowledges the Merck Graduate Fellowship in Analytical and Physical Chemistry. M.A.P.-S. thanks CONACYT (Grant Nos. 38507-E and 46556-Q).

Supporting Information Available: He I and He II close-up spectra of Cp*Ru(Pdl-C) (Figure S1), Cp*Ru((Pdl-N) (Figure S2), and Cp*Ru(Pdl-O) (Figure S3) and stacked He I close-up spectra of Cp*Ru(Pdl-C), Cp*Ru(Pdl-O), and Cp*Ru(Pdl-O*) (Figure S4). This material is available free of charge via the Internet at http://pubs.acs.org.

OM060100Z